Relaxation Time Measurements on Lipid-Peptide Systems

Marie Lundgaard Gudmundsson

1st June 2004

Bachelor Project

University of Copenhagen

Niels Bohr Institute

Membrane Biophysics and Thermodynamics Group

Supervisor: Thomas Heimburg

Abstract

In a theory proposed by T. Heimburg[1], it is shown that there is a proportionality between the heat capacity and the relaxation time of lipid membranes. This theory has previously been investigated experimentally for pure lipid systems, where the experiments were coexistent with the theory.

In this thesis, the theory is applied to pure lipid systems, as well as lipid-peptide systems. The relaxation of lipid membranes and of lipid membranes with an inserted peptide are investigated at temperatures close to the main transition. The investigation is done using pressure jump calorimetry.

The relaxation time and the heatcapacity are found to be proportional within error.

The theory underlying the experiments is presented, and the aspects of the phenomenon discussed.

This thesis is a bachelor thesis written during the spring 2004. The work was done during the spring 2004 in the Membrane Biophysics and Thermodynamics Group, Niels Bohr Instititue, University of Copenhagen.

The danish title is: Måling af relaksationstider for lipid-peptid systemer.

Marie Lundgaard Gudmundsson

cpr.nr. 120379-1204

Contents

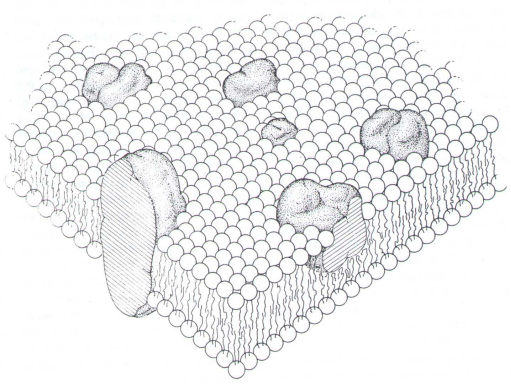

Figure 1.1: The Fluid mosaic model [2]

1 Introduction

In this section I will introduce some basic biological concepts necessary for an understanding of the project. Furthermore, I will motivate the investigations of the project.

1.1 Membranes of living organisms

1.1.1 Short introduction to the cell

Living organisms display a variety of cell types. There are cells that can exist on its own, such as bacteria, and there are the larger organisms, in which the different cell types depend on each other.

The boundary of the cell is defined by the lipid membrane. Inside the cell, there is a variety of organelles, proteins, nucleic acids and others, but it is beyond the scope of this thesis to discuss this. Yet, it is worth considering that many organelles of the cell are defined by membranes, such as the nucleus, mitochondria, Golgi apparatus and other.

1.1.2 The lipid membrane

The cell membrane mainly consist of lipids and proteins. The common view of biological membranes is based on the fluid mosaic model [2], in which the lipids form a homogeneous bilayer. Various kinds of proteins are embedded in this bilayer, and they can diffuse freely, see fig. 1.1. In this model, the lipid bilayer has no other function than acting as a matrix for the proteins, and provide a border between the interior of the cell and the surroundings.

A biological membrane consist of different kinds of lipids. In this thesis, I will be concerned with artificial membranes with only a single kind of lipid, in order to keep the system as simple as possible.

Lipids are amphiphilic molecules. The structure of a lipid is displayed in fig. **??**. The head group is polar and hydrophilic, whereas the nonpolar tails of fatty acids are hydrophobic. For different lipids, the headgroups may vary in size, charge and polarity. The tails may vary in number, length and degree of saturation.

Because of the amphiphilic nature of the lipids, they form aggregates when dispersed in water. One of the most important forms of lipid aggregates is the lipid bilayer. The lipid bilayer will tend to curve into vesicles. Examples of lipid bilayers can be seen in fig. 2.1.

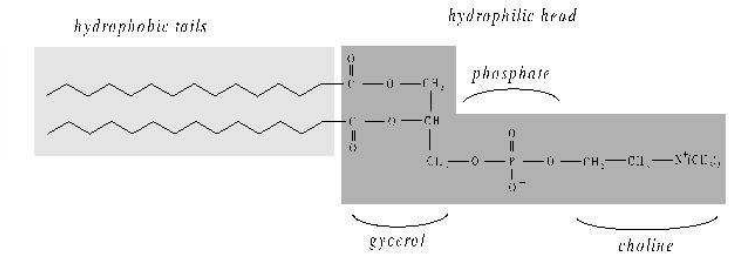

Figure 1.2: Structure of DMPC. Slightly modified after [7]

The lipid membrane can assume different configurations, depending of the temperature of the system. This will be discussed further in the Theory section2.1. The properties of the membrane are different for the different configurations, and thus the conditions for the proteins embedded in the membrane changes with temperature.

It is found, that the lipid membrane changes its state when changing the temperature in physiologically relevant temperature regimes (-20C to +60C).

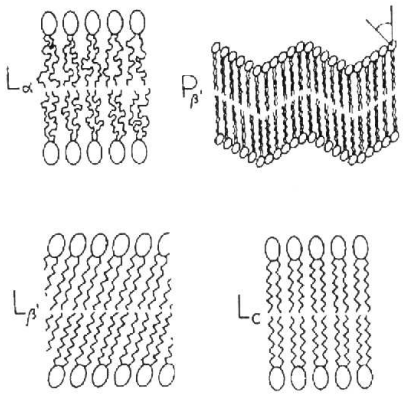

Figure 2.1: The phases of the lipid membrane [13]

2 Theory

First, I will consider the changes of the lipid membrane when undergoing a phase transition. Then I will give a short introduction to nonequilibrium thermodynamics, as this is the underlying feature of the theory on the relaxation kinetics of lipids. Afterwards I will consider the theoretical considerations underlying the experiments. In the end of this section, I will give a short outline of the application of the Ising model and Monte-Carlo simulations to phase transition of the lipid membrane. I will do this as the Monte-Carlo simulations give a picture of how the membrane changes during the phase transition.

2.1 Structural changes

2.1.1 Structure of the lipid membrane

In this thesis I will only consider one of the possible lipid aggregates, namely the lipid bilayer. The lipids used for our experiments are dimyristoylphosphatidylcholine molecules, in short DMPC. The strucure of DMPC is given in fig. 1.2. As seen, head group the DMPC molecules consist of a polar headgroup containing phosphate (negatively charged) and choline (positively charged). The headgroup is attached to glycerol, as are the two fatty acid chains. The hydrophobic fatty acid chains each consist of 14 C-atoms.

As mentioned in the Introduction, the lipid membrane can show different states, depending on the temperature. Considering the lipid bilayer, the different states occuring with increasing temperature are , fig. 2.1,

- L_c , crystalline
- L_β , "solid ordered", or "gel" phase. In this phase, the lipids are arranged in a in a 2-dimensional lattice. The chains are highly ordered, and tilted.
- $P_{\beta'}$,or "ripple phase". In this phase, the membrane are mainly in the gel state, but show line defects, which are desribed as "ripples". The lines have been contributed to alignment of fluid state lipids facing gel state lipids, which means that the thickness of the membrane is constant.

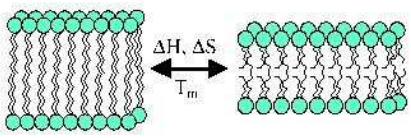

Figure 2.2: The change of the membrane at the maintransition [7].

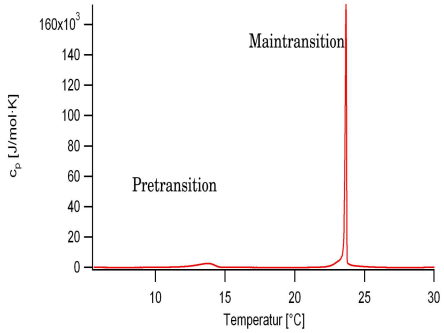

Figure 2.3: Heat capacity profile of DMPC

- L_α, "liquid disordered", or "fluid" phase. The lipids are randomly distributed in the membrane plane, and the chains are disordered.

In the temperature range of our experiments, we do not see the L_c phase.

2.1.2 Structural changes during phase transition

Now consider the tails of the lipids. In the gel phase, these have a high degreee of order. As the temperature increases, the energy of the system increases. This means that the fatty acid chains access more possible states, and they therefore become disordered. This causes the lipid membrane to decrease its thickness and increase its area, see fig. 2.2.

The heat capacity profile of a lipid membrane is shown in fig. 2.3. We see 2 peaks in the measured region. The first is known as the "pre-transition", a transition in which the membrane changes from the solid ordered phase to the "ripple-phase ". The second and much larger peak is the "main transition", in which the system changes from the "ripple-phase" to the fluid or liquid-disordered phase. This is the transition with which I will be concerned in this report.

2.1.3 The effect of gramicidin A

Gramicidin A is a transmembrane peptide forming pores in the membrane. It is assumed to be stable in lipid bilayers [7], and not to change its structure in the temperature range of our experiments. The only role of gramicidin A in the experiments considered here is to be embedded in the lipid membrane, in order to see how the insertion of a transmembrane peptide influences the heat capacity profile of the membrane. Thus, it can be considered a little, hard object in the lipid matrix.

2.2 Thermodynamics of the melting transition

We should now consider the lipid membrane in a thermodynamical context. The heat capacity is defined as

$$c = \frac{dQ}{dT}.$$

With the enthalpy defined as $H = U + PV$, one gets for constant pressure

$$c_p = \left(\frac{\partial H}{\partial T}\right)_p. \tag{2.1}$$

From this expression, one can determine the enthalpy by integrating over the temperature range of interest,

$$\Delta H = \int_{T_i}^{T_f} c_p dT,$$

where T_i denotes the temperature at the beginning of the phase transition, and T_f the temperature at the end.

Let us now consider the lipid system as an ensemble of degenerate states. For j states, the partition function is defined as

$$Z = \sum_j \exp\left[-\frac{\Delta H_j}{kT}\right]$$

For a system of j states, the thermal average of a quantity is given by

$$\langle A \rangle = \frac{1}{Z}\sum_j A_j \exp\left[-\frac{\Delta H_j}{kT}\right]. \tag{2.2}$$

By inserting eq. 2.2 into eq. 2.1, and differentiating with respect to temperature, one finds that [11]

$$c_p = \frac{\langle H^2 \rangle - \langle H \rangle^2}{RT^2} \tag{2.3}$$

Note the above eq. 2.3. This tells us that the higher the heat capacity, the higher the fluctuations in the system. At the temperature of a phase transition the heat capacity is high, and there will thus be considerable fluctuations in the system.

By similar considerations, it can be shown that the elastic constants are also related to the heat capacity [6] . The system is thus undergoing severe fluctuations in several variables in the course of a phase transition.

We now assume that the lipid system is very large, which is a valid assumption, and approximate the distribution af states around the equilibrium value with a Gaussian distribution. That is, we let

$$P(H - \langle H \rangle) = \frac{1}{\sigma\sqrt{2\pi}} exp\left(-\frac{(H - \langle H \rangle)^2}{2\sigma^2}\right), \tag{2.4}$$

where P is the probability of a state with enthalpy H. As σ for a Gaussian distribution equals $\langle H^2 \rangle - \langle H \rangle^2$, we find by the properties of the Gaussian distribution that

$$c_p = \frac{\sigma^2}{RT^2}. \tag{2.5}$$

Another relation [3] is

$$G\left(H - \langle H \rangle\right) = -RTlnP\left(H - \langle H \rangle\right) + const, \tag{2.6}$$

where G is the Gibbs free energy at enthalpy H. By inserting eq. 2.4 into the equation above, one gets

$$G(H - \langle H \rangle) = RT\frac{(H - \langle H \rangle)^2}{2\sigma^2} + const. \tag{2.7}$$

From the definition of the Gibbs free energy, $G = H - TS$, we find that

$$S\left(H-\langle H\rangle\right)=-R\frac{(H-\langle H\rangle)^2}{2\sigma^2}+\frac{(H-\langle H\rangle)}{T}+\frac{const.}{T}$$

Assuming that the system is very large, that is σ is very small, we approximate the above equation with

$$S(H-\langle H\rangle)\approx -R\frac{(H-\langle H\rangle)^2}{2\sigma^2}.$$

This result shows that the entropy is a harmonic potential of the enthalpy fluctuations in a large system, and this shall be used in deriving the relation between the heat capacity and the relaxation time.

2.3 Relaxation kinetics

In the pressure jump experiments, the system is perturbed form its equilibrium-position. In order to understand the reactions of the system to a pertubation, one have to consider some basic principles from nonequilibrium thermodynamics, which will be introduced in section2.3.1.

2.3.1 Nonequilibrium thermodynamics

The theory of nonequilibrium thermodynamics is necessary for an understanding of how a system will react to pertubations from equilibrium. As the system is perturbed from its equilibrium position, it will try to get back into equilibrium.

Consider a spring. When it is in its equilibrium position it will not move, but when stretched, it will oscillate back towards its equillibrium position, in the presence of friciton.

In a thermodynamical system, similar reactions occur. When we consider a system that is not in balance, there will be forces driving the system back to equillibrium. These are given by the theory of nonequilibrium thermodynamics[12]. The forces are defined as

$$X_i=\sum_j\left(\frac{\partial^2 S}{\partial\alpha_i\partial\alpha_j}\right)_0\alpha_j \tag{2.8}$$

These forces are thermodynamic forces. The $\alpha's$ indicate different fluctuating variables. The fluxes are defined as

$$J_i=\frac{d\alpha_i}{dt}=\sum_j L_{ij}X_j, \tag{2.9}$$

where the coefficient L_{ij} is a phenomenological coefficient. With these equations in mind, we are able to understand the reactions occurring when the system is perturbed from equillibrium.

2.3.2 Relaxation time and heat capacity

For lipid systems, it can be shown that the changes in area, volume and enthalpy are proportional [?, 4], and we therefore only have to consider the fluctuation of one variable, the enthalpy, that is $\alpha=(H-\langle H\rangle)$. The forces driving the system back to equilibrium, eq. 2.8, therefore reduces to

$$X(H-\langle H\rangle)=\left(\frac{\partial^2 S(H-\langle H\rangle)}{\partial(H-\langle H\rangle)^2}\right)_0(H-\langle H\rangle)=-\frac{R(H-\langle H\rangle)}{\sigma^2}$$

As there is only have one fluctuating term, one finds from 2.9, that

$$\frac{d(H - \langle H \rangle)}{dt} = -L \cdot \frac{R(H - \langle H \rangle)}{\sigma^2}$$

The solution to this is an exponential function, and we get

$$(H - \langle H \rangle)(t) = (H - \langle H \rangle)(0) \cdot exp\left(-\frac{R \cdot L}{\sigma^2} t\right) = (H - \langle H \rangle)(0) \cdot exp(-\frac{t}{\tau}) \tag{2.10}$$

As $\sigma^2 = RT^2 c_p$, eq. 2.5, and with use of the above eq. 2.10, we see that

$$\tau = \frac{\sigma^2}{R \cdot L} = \frac{T^2}{L} c_p = \alpha c_p \tag{2.11}$$

According to this expression, the relaxation time is proportional to the heatcapacity of the system in the final state. It is this theoretical result that I will test for lipid-peptide systems using calorimetric methods.

2.4 The Ising model and Monte-Carlo simulations

The Ising model is a two state model, developed by Ising in 1925, in order to describe ferromagnetic systems. However, the model can be applied to any two state system. One can apply it to a model of the lipid membrane, as it was first done by Doniach[8]. Using this model, one can make simulations on the lipid membrane in order to see how it fluctuates.

Without going into details, the basic principle of the Monte-Carlo simulations is the following:

1. Assume that each lipid can be in one of two states. Gel state with enthalpy H_g and entropy S_g, and fluid state with H_f and entropy S_f
2. Let the lipids be arranged on a two dimensional lattice, and determine the state of each lipid using a randum number generator.
3. Determine the interactions and energy differences of the different states, and construct the Hamiltonian of the system.
4. Determine the probability of finding a lipid in a certain state, depending on the state of the surrounding lipids.
5. Pick a random lipid. Determine the probability of finding the lipid in gel state and fluid state, and determine wheter to change the state of the particular lipid by using a random number generator.
6. Perform step 5 again.

See for instance [7, 5] for more details on the application of Monte-Carlo simulations on lipid-peptide systems.

In the above approachs, we assume that each membrane lipid can be in one of two states, either gel or fluid. This is an assumption, as it is diffucult to say exactly when a lipid is best described as "gel" or "fluid". Yet, it shows that the two state model is a very good method for describing cooperative phenomena [14]. It will not provide any detailed information on the conformation of the chains during the transition, but one can get intermediate values by averaging over the vaules.

A more precise model is the ten state model developed by Pink et. al [9]. For our purpose, however, the assumption of the two state Ising model is very suitable.

The advantage of the Monte-Carlo simulations in this context, is that it provides a picture of how the different lipid states are distributed in the membrane, and a picture of how the membrane is constantly fluctuating. Thus, the Monte-Carlo simulations provides a good picture of how the lipid membrane changes during the phase transition.

In the first picture shown in figure 2.4., we simulate a lipid membrane in equillibrium at a temperature $T_i = T_m - 0.5K$, where T_m is the melting temperature. The membrane is found to be almost entirely in the gel state. The temperature is now shifted instantaneously to $T_f = T_m + 0.5K$. The snapshots show how the system evolves towards the new equillibrium.It is interesting to se how the lipids in the two different states tend to form domains. Also, it gives an intuitive picture of the cooperativity of the membrane.

One can compare the picture provided by the Monte-Carlo simulations with the picture obtained when assuming that the lipids melt independetly of each other. This would yield the equillibrium constant of reaction

$$K = \exp\left[-\frac{\triangle G_{melting}}{RT}\right].$$

From this, one can calculate the transition halfwidth of a phase transition of a lipid membrane. When assuming that the lipids melt independently, the transition halfwidth is found to be several ordes of magnitude higher than the one of the pronounced peaks measured in experiments.

This is because of the cooperativity of the lipid membrane, that is the lipids do not melt indepently of each other. A solid lipid surrounded by liquid molecules is more likely to melt, than a solid lipid surrounded by other solid molecules.

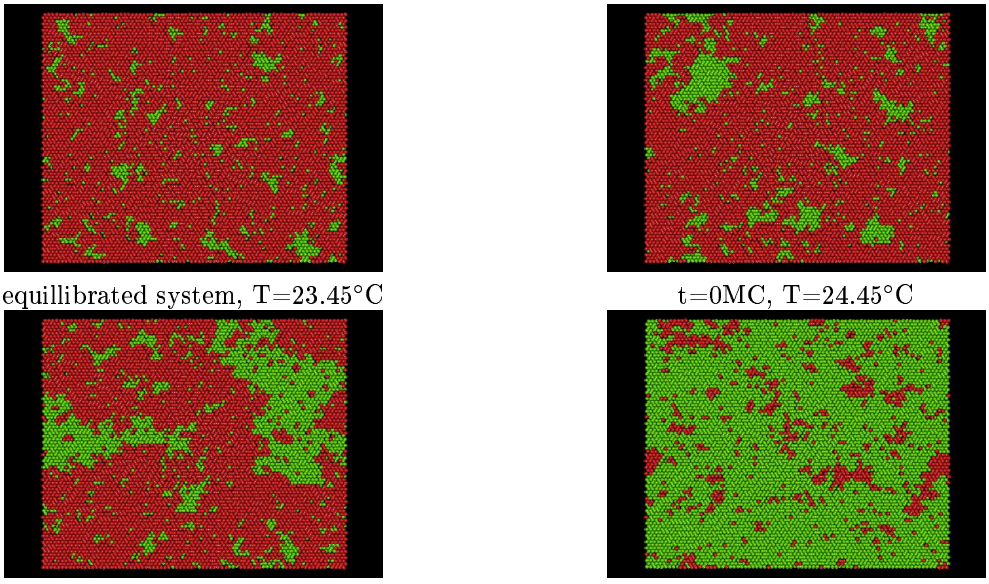

Figure 2.4: Snapshots from Monte-Carlo simulations on a lipidsystem
The system was equlibrated at a temperature 0,5K below the melting point. The red points denote lipids in gel-state, and the green points lipid in the fluid state. At t=0, the temperature T was increased by 1K. The pictures show the membrane in the equillibrium state, at t=0, t=500MC-cycles and t=1700MC-cycles. (H. Seeger, Max-Planck Institute for biophysical Chemistry, Göttingen and Niels Bohr Institute, Copenhagen, unpublished results).

3 Materials and methods

In this section, I will explain how the samples were prepared, and how the experiments were conducted.

3.1 Preparation of samples

The following simple equations are used for calculating the concentrations:

$$m = n \cdot M_w$$

and

$$n = c \cdot V$$

M_w denotes the molar weight, n the moles and m the mass. V denotes the volume and c the concentration of the sample.

3.1.1 Buffer

We use a buffer solution to keep the conditions of the sample constant throughout the experiments. The buffer used kept the sample pH-value constant, and prevented the growth of bacteria in the sample.

The pH-value should be kept constant, as a change of pH may change the properties of the membrane. We used Hepes, as this buffers around pH=7. The growth of bacteria has to be prevented, as bacteria may destroy the membranes. EDTA is therefore added to the buffer. EDTA binds calcium, and as bacteria require calcium, the addition af EDTA prevents the growth of bacteria.

Hepes is an abbreviation for 4-2-hydroxyethyl-1-piperazineethanesulfonic acid. The Hepes used was ordered from Sigma-Aldrich (St. Louis/MO, USA). EDTA is an abbreviation for ethylenediaminetetraacetic acid. The EDTA used was ordered from Fluka (Buchs, Switzerland).

We prepared a buffer of 10mM Hepes, 1mM EDTA, ph=7.

The buffer was prepared by calculating the needed amounts of Hepes and EDTA. The calculated amounts of Hepes and EDTA was dissolved in distilled water. Thereafter the pH was measured, and the pH adjusted to pH=7 by addition of 1M NaOH and 0,1M HCl. This has a slight influence on the concentration of Hepes and EDTA, but as the added amounts are very small compared to the amount of buffer, one can neglect that. Also, we do not need the value of the buffer concentration in any calculations, we only need the buffer to be a constant throughout all of the experiments.

3.1.2 DMPC-vesicles

For the preparation of the DMPC-samples, the procedure is the following. We used lipids purchased form Avanti Polar Lipids (Alabaster/Al, USA) without further purification.

The amount of lipid needed is calculated. One should start with preparing a concentrated solution such as 100mM, and then later dilute this solution, as the different experiments are conducted with samples of different concentration.

The needed amount of lipid is dissolved in the buffer. The solution is stirred using a magnetic stirrer, and heated to a temperature above the melting point of the lipids. By simply dissolving the lipids in the buffer at a temperature above the melting point, the DMPC selfassembles into multilamellar vesicles. The sample is kept in the fridge for at least 3 days before it is used for measurements, as the vesicles tend to swell for a period after the preparation. The swelling of

the vesicles will broaden the heat capacity profile of the solution, as the cooperativity decreases with larger surface.

A pure DMPC sample was prepared and kept in the fridge.

3.1.3 Addition af gramicidin A into the lipid membrane

The preparation of the samples with gramicidin A is slightly different. One starts with calculating the appropriate amounts of lipid and gramicidin A. The gramicidin A used is from bacillus brevis, and is purchased from Fluka (Buchs, Switzerland).

The amount of gramicidin A in the final sample is given in "mol-percentage". In this thesis, the mol-percentage is defined in the following: A sample with 1 mol-% gramicidin A containing 100mol of lipid, contains 1mol of gramicidin A. That means, the mol-percentage indicates the number of moles of peptide compared to the number of moles of lipid.

Gramicidin A is a transmembrane molecule. In order to insert the gramicidin A into the membrane, we used the following procedure: The lipid was dissolved in an organic solvent. We used a 2:1 dichloromethane/ethanol-mixture. The gramicidin A was dissolved in the same kind of solvent, and then added to the lipid solution.

The sample consisting of lipids, gramicidin A and organic solvent was dried with nitrogen and thereafter left under vacuum over night with the pump working, to ensure that all solvent was removed.

This procedure works because the molecules in the gas phase are in equilibrium with the molecules in the fluid phase. As the sample is vaporized with nitrogen, some of the organic molecules will go into the gas phase in order to establish this equilibrium. These molecules are removed with the nitrogen leaving the sample. As new nitrogen is provided constantly, there will be a constant flux of organic molecules out of the solution. The same principle is removing the organic solvent molecules when the sample is left under vacuum.

The obtained sample now consist of lipids and gramicidin A in a fixed relationship. This can now be used to prepare a solution of vesicles, as described in Sec. 3.1.2.

Samples with 0.5mol%, 1mol% and 1,5mol% gramicidin A were prepared. The three samples were kept in the freezer until they were needed. This was done as a to prevent growth of bacteria in the samples.

3.2 Differential scanning calorimetry

The calorimeter used for the measurements is a differential scanning calorimeter, type VP-DSC, produced by Microcal (Northhampton/MA, USA). The calorimeter is operated via a computer.

The calorimeter has two cells, and the temperature of these two cells can be controlled to high precision. When conducting the experiments, one cell is filled with the sample, and the other with a buffer solution.

The calorimeter has two different scanning-modes. The "isothermal mode" where it maintains a certain temperature, and the "scanning mode" where it continuously changes the temperature in a given temperature-interval.

The basic principle of the calorimeter is that it maintains the temperature difference of the two cells at zero. The power difference is recorded throughout the scan, at a sample rate controlled via the computer. The excess power supply of the sample cell compared to the reference cell, is called the excess power, ΔP. The excess heat added to the sample cell is then found by integrating the excess power supply with respect to time,

$$\Delta Q = \int_t^{t+\Delta t} \Delta P(t')dt' \cong \Delta P \cdot \Delta t. \tag{3.1}$$

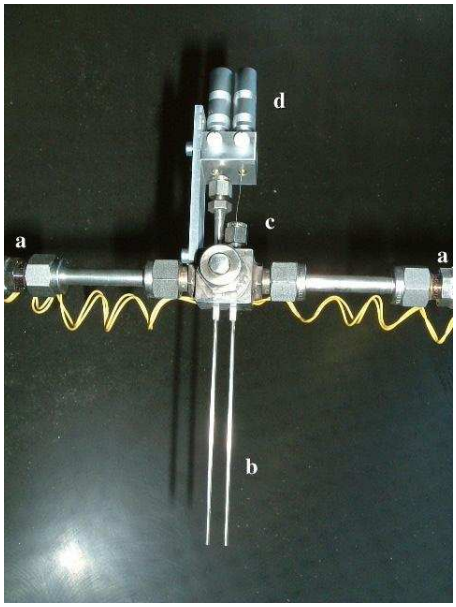

Figure 3.1: The Pressure cell
a: the magnetic valves. The nitrogen pressure is applied from the left valve, and released from the right. **b**: the two cells. The left cell contains the sample, and the right cell the reference buffer solution. **c**: the openings through which the sample is injected. **d**: The thermocouples. These are not a part of the experiments considered in this thesis.
Not in the picture is the opening for the device that measures the pressure.

3.2.1 Heat capacity profiles

When measuring the heat capacity profiles, the calorimeter i run in scanning mode. Let the excess heat capacity be given by

$$\Delta C_p = \frac{\Delta Q}{\Delta T}$$

where ΔT is the increase in temperature.

As the calorimeter raises the temperature from T_i to T_f, it measures how much energy is added to the two different cells. The temperature is measured at a scanrate given by $\frac{\Delta T}{\Delta t}$. Combining the excess heatcapacity with eq. 3.1, the excess heatcapacity is computed by

$$\Delta c_p = \frac{\Delta P}{\left(\frac{\Delta T}{\Delta t}\right)}.$$

Mesurements of heat capacity profiles can be seen in the Results section.

The heat capacity profiles were measured on 10mM sample solutions, filled directly into the calorimeter cells.

3.2.2 Pressure jump experiments

For the pressure jumps, we use a special self constructed device, a "pressure cell". It has two cells that fits into the two calorimeter cells, fig. 3.1. Before the pressure cell is inserted into the calorimeter, the calorimeter cells are filled with distilled water. This is done to ensure a continous transfer of heat to and from the pressure cell, and to get a precise measure of the temperature of the pressure cells.

Once inserted to the calorimeter, the pressure cell is connected to a pressure supply. We used nitrogen in a pressure bottle mounted with a pressure reducer to control the pressure applied. In our experiments we apply a pressure of 40bar to the system. The intake and release of nitrogen is controlled by two magnetic valves, which are controlled via a computer. The

valves are coaxial valves, produced by Nova Swiss (Effretikon, Switzerland). The computer controlling the valves is another than the computer controlling the calorimeter.

Prior to the pressure jumps, the temperature at which we want to measure is specified via the computer that controls the calorimeter. The calorimeter now adjusts to the specified temperature. The jumps are started when the system has reached equilibrium.

When doing the pressurejumps, the system undergoes 2 positive and 2 negative pressure jumps of 40bar each. Between each jump, there is a pause of 5 minutes, to allow the system to stabilize at the new equlibrium. Furthermore, the pressure cell is connected to a pressure gauche that measures the pressure, produced by Nova Swiss (Effretikon, Switzerland). The pressure is recorded by the program that controls the valves.

The filling of the pressure cell is somewhat difficult. The two cells are very narrow, and only exactly allows the syringe used for the filling to fit in. One therefore has to be very careful when filling it, in order not to "press out" the already filled solution with the syringe. The cells were filled by adding the solution in smaller portions, and stirring the solution in the cell with a very thin metal wire in between. The stirring prevents aircushions in the cell.

We know how much solution we fill into the cell, but we do not know how it is distributed in the cell. This, however, does not effect the shape of the profiles, as these depend on composition of the solution.

The pressure jumps were conducted on 50mM samples, except for the sample with 0,5mol%-gramicidin A, which were conducted on a 75mM solution. The concentration of the solution has influence on the strength of the response to a pressure jump. The strength of the jumps are of importance in the analysis of the data, as will be discussed in the Results section.

3.3 General concerns about the experiments

It is very important that the samples stays the same throughout the experiments. When preparing the samples, all necessary equipment should be cleaned thoroughly. We used distilled water, mucasol, and ethanol for the cleaning of the equipment, and afterwards it was dried with nitrogen. The glasses containing the samples were sealed with a lid and parafilm.

The calorimeter was cleaned between the heat capacity measurements directly in the calorimeter cells. This was done by rinsing it out with water, mucasol and ethanol. After measurements using the pressure cell, only water had been filled in to the calorimeter cells, and so it was only cleaned with water. After both cleaning procedures, it was dried using nitrogen.

When kept outside the calorimeter, the pressure cell had the opening for the pressure measuring device sealed with parafilm. The openings for the pressure intake and release were closed with the magnetic valves and metal lids.

4 Results

In this section I will analyze the results obtained in our experiments. First I will give a short introduction to the fitting/analysis-procedure, and afterwards, I will display the results obtained.

4.1 Analyzing the data

All data from the calorimeter was written to data files on a computer through a computer program designed by the manufacturer of the calorimeter.

The analysis of the obtained data was done with the program Igor Pro by Wavemetrics.

4.1.1 Heat capacity profiles

When operating the calorimeter in scanning mode, see sec. 2.2., the experiments provide us with knowledge of how the heat capacity of the specific sample changes with respect to temperature, compared to the heat capacity of the reference.

As

$$c_p = \left(\frac{\partial H}{\partial T}\right)_p,$$

one can determine the enthalpy by integrating over the temperature range of interest,

$$\Delta H = \int_{T_i}^{T_f} C_p dT.$$

By integrating over the temperature range of transition, we get the transition enthalpy.

When analyzing the heat capacity profile, one has to do a base line correction, in order to let the excess power outside the main transition approach zero. This is done to distinguish the main transition from other relaxations.

In order to include the whole transition in the calculation of the transition enthalpy, one should be careful to start the integration outside the transition, so that the excess power supply, theoretically, is zero at T_i and T_f.

We define the melting temperature as the temperature at which half of the lipids are in gel state and half of the lipids in fluid state. Assuming that the distribution is gaussian, the melting temperature is the temperature at which c_p is a maximum.

4.1.2 Pressure jump experiments

In the pressure jump experiments the calorimeter is run in the isothermal mode. When we apply pressure, this corresponds to an increase of the transition temperature [4], see fig. 4.1. If the state of the lipidsystem is thereby changed, that is, the amount of molecules in liquid/gel-states are changed, the calorimeter will have to add/subtract heat from the system, in order to keep the temperature constant.

A typical pressure jump experiment in the range of transition is shown in fig. 4.2. Here the scan is performed at 23.74°C. At the beginning of the scan, there is an applied pressure of 40bar, and the sample is in the gel state. The first peak is the response to the release of pressure. The applied pressure of 40bar is released in approximately 10ms. The release of pressure shifts the melting temperature towards a lower temperature. At a temperature of 23.74°C and no additional pressure, the sample is in the main transition. Part of the lipids in the sample now melts, a process which consumes heat. As the calorimeter is in the isothermal mode, the calorimeter adds heat to the sample in order to keep the temperature constant. Note

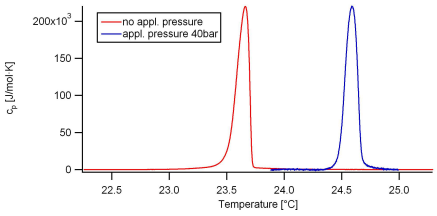

Figure 4.1: The heat capacity profile of DMPC measured with and without additional pressure

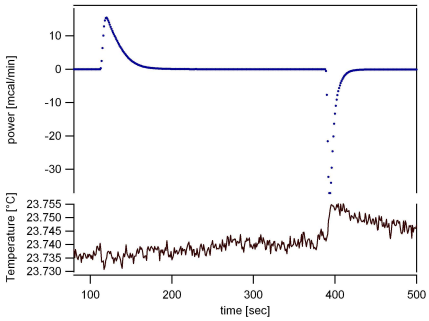

Figure 4.2: Experimetal output of a pressure jump experiment performed at 23.74°C

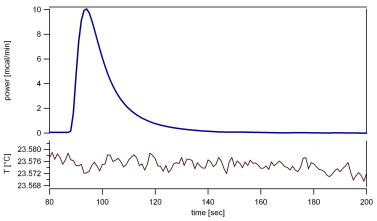

Figure 4.3: Experimental output of a pressurejump in the range of transition, T=23.57°C

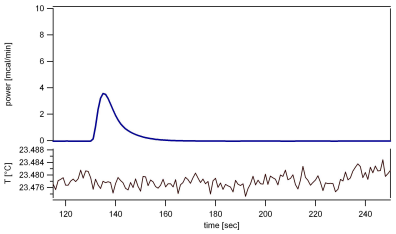

Figure 4.4: Pressurejump outside the range of transition, T= 23.48°C

that the temperature is only fluctuating in the third decimal, see fig. 4.3. After equilibration of the system, a pressure of 40bar is applied to the system. This means that the opposite reaction occurs, the temperature of 23.74C now corresponds to the system being in the gel state. There is thus a release of heat as the lipids change from fluid to gel. The calorimeter therefore cools the sample, in order to maintain the temperature constant. As seen in fig. 4.2., the calorimeter is not able of keeping the temperature constant to the same degree of precision as for the negative pressure jump. This is due to the fast relaxation, and the fact that the calorimeter is not as efficient in cooling as in heating.

4.1.3 Model for the calorimeter output

Assume first that the system is at a temperature at which a pressure jump will not cause a change of the state of the lipids in the system.

Being outside the range of transition, one would not expect any signal. There is one, however, and we contribute this to the experimental setup, and call it the "water response".

We describe the propagation of the signal from the water to the detecor of the calorimeter with a model containing 2 processes of heat transfer:

$$\begin{array}{ccccccc} x(t) & & l & & y(t) & & m & & z(t) \\ water & \longrightarrow & & cell & wall & \longrightarrow & & detector \end{array} . \tag{4.1}$$

The factors l and m are thus constants of the instrument. The two processes can be desribed with three differential equations:

$$\begin{aligned} \dot{x}(t) &= -l \cdot x(t) \\ \dot{y}(t) &= l \cdot x(t) - m \cdot y(t) \\ \dot{z}(t) &= m \cdot y(t) \end{aligned}$$

With the appropriate boundary conditions $x(0) \neq 0$ and $y(0) = 0$, one finds for x(t) that

$$x(t) = c_1 \cdot e^{-l \cdot t}$$

and that

$$y(t) = c_2 \cdot \left(e^{-m \cdot t} - e^{-l \cdot t}\right).$$

Because of the relation between $y(t)$ and $\dot{z}(t)$, one gets the detector signal as

$$z(t) = c' \cdot \left(e^{-m \cdot t} - e^{-l \cdot t}\right) \tag{4.2}$$

As mentioned above, we assume that there is no contribution to the detector signal from the lipids when we are well outside the range of transition. The values of l and m are therefore obtained by doing pressurejumps at temperatures far away from the range of transition, and fitting the responses with the Eq. 4.2.

When we are in the range of transition, we assume the following scheme

$$lipid \xrightarrow{k_{lipid}} water \xrightarrow{l} cell\ wall \xrightarrow{m} detector \ . \tag{4.3}$$

The signal recorded by the calorimeter, the calorimeter response, will now consist of a contribution from the lipids convoluted with the instrument response. Since we want to analyze the contribution from the lipids, we will have to distinguish this from the instrument response. This is done by interpreting the recorded data from the calorimeter in the following way:

Let the signal be the sum of the water response, and a contribution from the lipid. The contribution from the lipid is delayed compared to the water response. The lipid response is described as a convolution of rectangular impulses at different times during the relaxation period. Mathematically, one describes the calorimeter response as

$$P_{cal}(t) = \int_{\tau=0}^{t} P_{lipid}(\tau) \cdot R_{instr}(t-\tau) d\tau + z(t). \tag{4.4}$$

$R_{instr}$is the response of the instrument on the lipid response, and is described in the same way as the water response, z(t). It is assumed that the lipid response is described by a single relaxation process with an exponential decay;

$$P_{lipid}(t) = P^0_{lipid} \cdot e^{-k_{lipid} \cdot t}. \tag{4.5}$$

The program fits the experimental calorimeter response to eq. 4.4. The fit parameters are P^0_{lipid}, k_{lipid} and c', the amplitude of z(t). Note that $\tau = \frac{1}{k_{lipid}}$. Besides providing the values of the different rate constants, the program generates the values of the standarddeviation of the relaxation time τ, and the temperature T. The program also generates the areas of the total and water contributions to the signal. The areas of the fit of total - and water contribution are calculated, and displayed as A1 and A2.

Be aware of the fact that the word "water response" may be misleading. Included in the water response are also relaxations with relaxation times to fast and contributions to small to be resolved by the calorimeter.

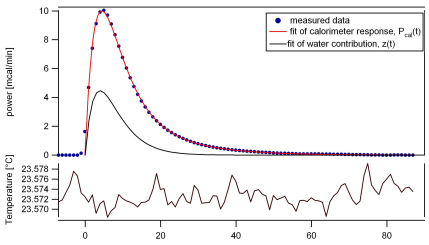

Figure 4.5: Calorimeter response and fit of a negative pressure jump performed at DMPC sample at T=23.57°C

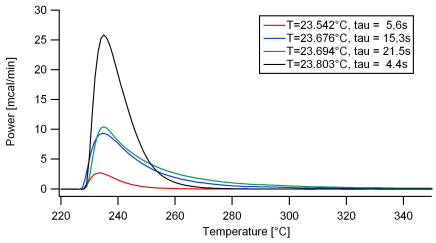

Figure 4.6: Calorimeter response for negative pressure jumps conducted at temperatures around the heat capacity maximum.

The program uses the standard χ^2-method to fit the curve.

An example of a fit of a pressure jump can be seen in fig. 4.5. The figure shows the fit of eq. 4.4. to the experimental output, and the calculated water contribution, eq. 4.2.

In fig. 4.6. it is seen how pressure jumps at temperatures around T_m yields different relaxation times.

Concerns about the fitting procedure

When fitting the data of a single pressure jump, one has to specify in which range the fitting should take place. One should try to fit from the beginning of the jump, to the point where the system is again in equilibrium.

Furthermore, the model is based on some assumptions about the system, and one has to consider whether these assumptions are valid for the particular pressure jump.

- We assume that the system after the jump is at a specific temperature. The relaxation time depends on the temperature, and if the temperature changes during the relaxation process, so does the relaxation time. One therefore has to observe the fluctuations of the temperature during the jump.
- We assume a small perturbation from equilibrium. In the high temperature limit of the jumps, i.e. when the system jumps into the fluid region, the system undergoes a large pertubation. This means that we are at the edge of the model conditions.

One should therefore always judge whether the conditions for the theory to be applied is fulfilled for each pressure jump.

4.2 Data

In the following, I present the results of the experiments.

4.2.1 C_p-profiles

The heat capacity profiles of 10mM solutions of a pure DMPC-sample, and 10mM DMPC-samples with 0,5mol%, 1mol% and 1,5mol% gramicidin A have been measured. The scan rate has been 0,5-1 degree/hour, and were thus conducted over night. When in scanning mode, one has to do relatively slow scans, in order to get precise profiles. At high scan rates, the temperature changes fast. This means that one gets signals at T_1 which are a contribution from the sample at T_2, due to relaxation processes to slow for the scan rate.

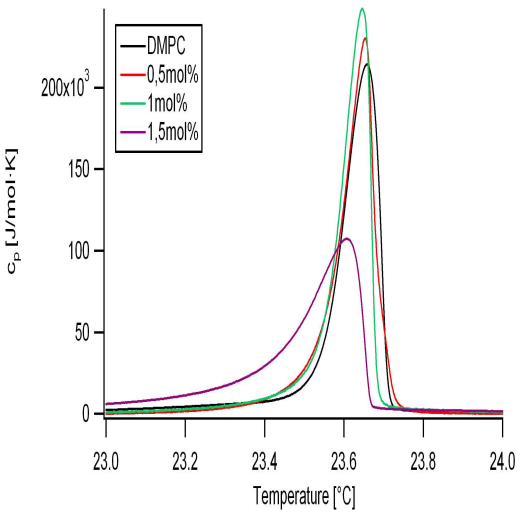

Figure 4.7: Normalized heat capacity profiles. DMPC with 0-1,5mol% gramicidin A.

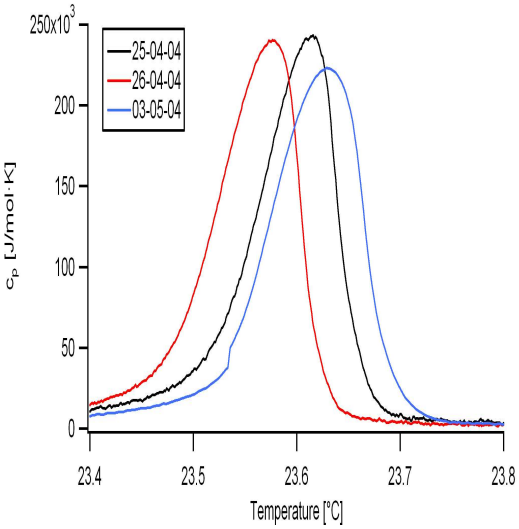

Figure 4.8: The shift of the melting point at different dates. Profiles for DMPC with 0,5mol% gramicidin A.

The enthalpy of the main transition was measured for each scan, and the curves were rescaled to yield the tablevalue of the transition, $26300\frac{J}{mol}$ [10]. As the amount of gramicidin A is very small compared to the amount of lipid, and more important that it is assumed to be stable in the temperature regime in which the measurements are done, it is reasonable to neglect the contribution from this in the evaluation of the transition enthalpy.

In fig. 4.7., the measured heat capacity profiles are displayed. For the sample containing 1,5mol% of gramicidin A, it is obviously seen that the insertion of gramicidin A into the membrane lowers and broadens the c_p-profiles. For the samples containing 0,5mol% and 1mol% gramicidin A, we observe a slightly higher heat capacity maxima than for the pure DMPC heat capacity profile.

It seems that there is a slight lowering of the melting point of the lipid membrane upon addition of gramicidin A. The gramicidin A is a transmembrane peptide shorter than the thickness of the lipid membrane. As the fluid state lipids are shorter than the gel state lipid, one would therfore expect that addition of gramicidin A would favor the fluid phase [5].

The heat capacity profiles of the samples were also measured in the pressure cell. Here we saw a shift of the melting point of ~0.04K, from the measurements directly in the calorimeter. This is most likely to be attributed to the fact that the lid used when measuring directly in the calorimter contributes with an additional pressure of appr. 50psi. Further, there was a slight difference in the shapes of the profiles measured directly in the calorimeter, and in the pressure cell.

The heat capacity profile of each sample was measured several times in the pressure cell. We observed a shift of the melting temperature over time. An example is showed in figure 4.8. That is, the melting point shifted, although the sample was kept in the cell all the time. The shape of the profiles stayed the same, except for a slight broadening due to swelling of the vesicles.

The shifts can be due to several reasons:

- The density of the lipids used are higher than the density of the buffer, and the vesicles will therefore tend to sink. One could therefor imagine that the vesicles, with time, might

form aggregates with a lower melting temperature. This is however, not very likely, as the profiles shifted towards both higher and lower temperatures.

- There might be bacteria in the samples, which may influence the membrane strucure in a way that shifts the melting temperature. This is probably not the reason. One would expect that bacteria have a larger influence than shifting the profile. Rather, bacteria would destroy the membrane, and the profile would have been changed to a larger degree.
- The conduction of the pressure jumps may have an influence on the vesicles. The pressure is applied with nitrogen, and the nitrogen might have an influence on the membranes. There are being made preparations for experiments with argon as a pressuresupply in the group, in order to see whether it is the nitrogen that has an influence on the system.
- The temperature scale of the calorimeter might be unstable, that is the temperature scale of the calorimeter is not properly calibrated. In the same period as I used the calorimeter, other group members have reproted "strange" results from the calorimeter.

I would consider the last explanation as being the most likely, as the shifting did not show systemacy, but shifted the melting point towards both higher and lower temperatures. The fact that the profiles were not altered significantly also favors this explanation.

As seen in fig. 4.8., the shifting of the melting point from day to day was within 0.1K, which may seem as a minor variance. But as the transition half width measured also is approximately 0.1K, this is a significant change. The pressure jumps have to be performed close to the melting point in order to let one interpret the results with respect to the theoretical assumptions. Thus, a precise knowledge of the position of the melting point is necessary. The heat capacity profiles were therefore measured as close to the conduction of the pressure jumps. That is, the heat capacity profiles were most often measured in the pressure cell the over night, before conducting the pressure jumps.

The response of C_p-profiles to pressure

We measured the response of the heat capacity profile to applied pressure. The melting point of the lipid changed from $T_m = 23.66°C$ to $T_m = 24.59°C$, that is $\Delta T = 0.93K$, see fig. 4.1. As seen the profile changes a bit. This is due to the fact that there was a leak in the system, which means that the pressure did not stay constant, and the shift therefore was not constant. The scan was done overnight, and the pressure shiftet from 40.2bar to 40.6bar. There has most likely been smaller fluctuations in the pressure during the scan, and the small change in the profile is then due to a minor fluctuation while passing through the transition.

We assume that there is a linear relationship between the applied pressure and the temperature shift [4]. With the data obtained in the experiment shown in fig. 4.1., we find the relation between the temperature without applied pressure and the corresponding temperature for a system with an applied pressure p to be

$$T_{\Delta p=0} = T_{\Delta p=p} - 0.93K \cdot \frac{p}{40bar}. \tag{4.6}$$

4.2.2 Pressure jumps

According to the theory, the relaxationtime is given by eq. 2.11.;

$$\tau = \frac{\sigma^2}{R \cdot L} = \frac{T^2}{L} c_p = \alpha c_p,$$

that is, the relaxation time depends on the heat capacity and the temperature in the final state. We are therefore only concerned with the jumps into the phase transition. For jumps

out of the phase transition, we would only expect very fast relaxationtimes, which are to fast to be resolved from the calorimeter signal by the fitting procedure. But by observing the pressure jumps in fig. 4.2, one sees that the system comes to equillibrium faster in the positive pressure jumps than in negative. As the heat uptake and release in the two different jumps theoretically are equal, one also observed a higher amplitude for the positive pressure jumps, but a faster relaxation time.

Each pressure jump has been analyzed and fitted according to the procedure described in Sec. 4.1.2.

For measurements well inside the range of transition, the fitting procedure generally resulted in good fits. That is, the calculated curve fitted well with the experimental data, the standard-deviation of τ was rather small, and a small variation of the starting point of the fit did not effect the calculated numbers significantly.

However, for pressure jumps performed at temperatures at the boundaries of the transition, the fitting were somewhat more difficult. This is due to several reasons:

- Below the melting point, the pertubation of the system is very small, and the contribution from the lipids to the response is therefore also small. The model is valid at this point, but the signal in this region is rather weak compared to the noise. It is not possible to give a trustworthy fit in this region. This is indicated by the fact that a slight change of starting point may result in big deviations of the calculated numbers.

- Above the meltingpoint, the system undergoes a large change. This results in a major output of energy, and may often result in "distorted" relaxation curves. The output from the calorimeter can in these cases not be fitted by Eq. 4.5. Because of the big release of heat, the calorimeter cannot keep the temperature constant, and we therefore have a situation where the value of τ changes during the relaxationprocess.

Positive pressure jumps

For temperatures above the melting point, where the fitting can be difficult as described above, one can obtain relaxation times by performing positive pressure jumps. One then adjust the temperature such that the system without applied pressure is in the fluid state. When the pressure is applied, the system undergoes a transition towards the gel state. Thus, heat is released from the sample, and this is subtracted by the calorimeter, causing a negative calorimeter response.

When comparing the relaxation times resolved from the positive pressure jumps to the heat capacity profile measured without applied pressure, one has to shift the temperature of the measured relaxation time with resprect to the applied pressure, by using eq. 4.6.

An inconvenience of the positive pressure jumps is that the calorimeter does not subtract heat from the sample as effectively as it adds it. This means that the temperature fluctuates more during a positive jump than during a negative jump. In fig. 4.2., one sees that the temperature has a tendency to increase after a positive pressure jump. This is a violation of the condition that we need a well defined system in order for the fitting procedure to yield correct values.

As the theory states that the relaxation time is only dependent on the state of the system after the perturbation, one should try to determine this as good as possible. Therefore the positive pressure jumps were only conducted as a supplement to the negative ones, as the negative ones are jumps into a more well defined state.

Relaxation times

Investigation of the relation between the relaxation times and the heat capacities is the main aim of this thesis. In figures 4.9-4.12, I have plotted the heat capacity profiles and the relaxation times of the different samples. As described in Section 4.2.1, there was a shift of the heat capacity profiles over time. I therefore tried to measure the profiles directly before conducting the experiments. This was done because the conduction af the pressure jumps take some time, and a covering of the whole transition would take several days, in which the profile might shift.

I have compared the relaxation times measured at a given day to the most recent heat capacity profile. I have compared the particular heatcapacity profile to the profile measured for the 10mM solution in the calorimeter. In the figures 4.9-4.12, the relaxationtimes are measured at different days, but all shifted in accordance with the procedure just described.

There is some scattering in the relaxation times, especially for the first 3 samples. That is due to uncertainties in the fitting procedure, and the shifting of the melting point, although I have tried to correct this. The fourth figure, fig. 4.12, showing results for the sample with 1,5mol% gramicidin A, shows relaxation times measured at the same day. One sees a much lower scattering in the relaxation times compared to the three other samples.

4.3 Proportionality between heat capacity and relaxation time

Determination of α and L

The factor α was found to be given by eq. 2.11

$$\tau = \frac{\sigma^2}{R \cdot L} = \frac{T^2}{L} c_p = \alpha c_p \Rightarrow \alpha = \frac{\tau}{c_p} = \frac{T^2}{L}.$$

As we only consider the lipid to give a contribution to the relaxation, we would expect L and α to be constant for the four different samples. The errors in α and L are calculated by the use of error propagation. This is done as c_p and τ_{max} are determined from different experiments, and thus are independent variables. That is

$$\delta\alpha = \sqrt{\left(\frac{\partial\alpha}{\partial\tau}\delta\tau\right)^2 + \left(\frac{\partial\alpha}{\partial c_p}\delta c_p\right)^2}.$$

I have determined the values from the data at the heat hapacity maximum. The data are obtained form the datasets displayed in figures 4.9 - 4.12., and listed in table 4.1.

The uncertainty of the measured relaxation times are a rough estimate based on the scattering in values around the melting point. The uncertainty in the value of c_p is estimated to be 5%. The uncertainty in T_m is estimated to be 0.05K. This is based on the shifting of the profiles over time.

As mentioned in sec. 4.2.1, there was a shifting of the melting point over time. In the determination of α and L, I use the meltingpoint found when measuring the heat capacity profile in the calorimeter.

The values of L and α obtained from the experimental data are displayed in table 4.2.

The phenomenological constants are found to be proportional within error. The α-values are nearly identical within the experimental error.

The samples with 0,5 - and 1mol% Gramicidin A showed a larger maxima of the heat capacity as did the pure DMPC sample, but lower relaxation times. Yet, there is some scattering in these values, and one can conclude that the four different samples yield α-values which are very similar when taking the experimental error into accouont.

Thus, it is found experimentally that there is a proportionality between the heat capacity and the relaxation time.

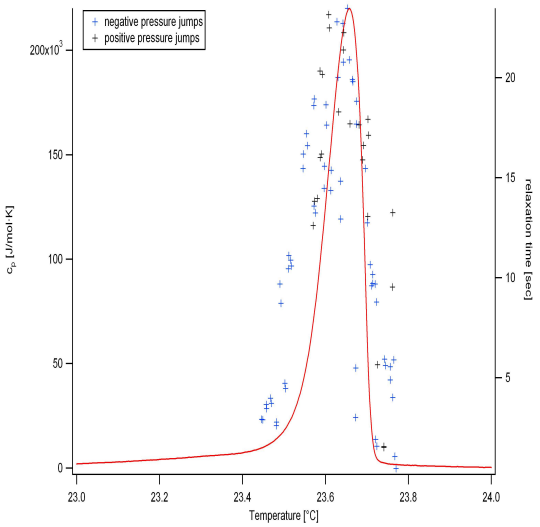

Figure 4.9: Pure DMPC

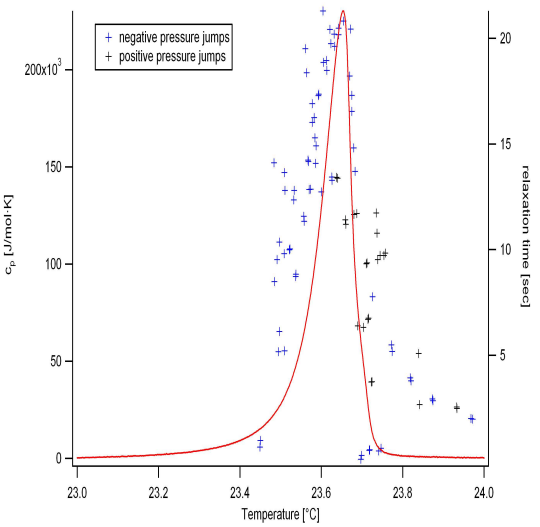

Figure 4.10: DMPC with 0,5mol-% Gramicidin A

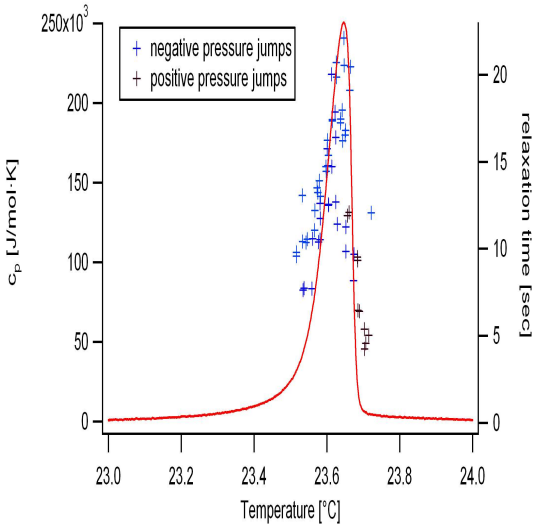

Figure 4.11: DMPC with 1mol-% Gramicidin A

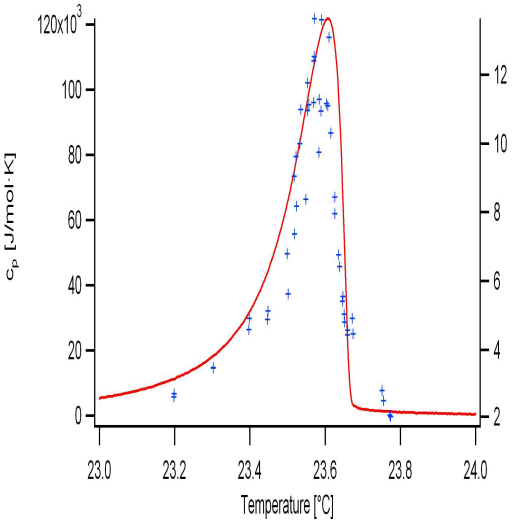

Figure 4.12: DMPC with 1,5mol-% gramicidin A

Sample	T_m[K]	$c_{p,max}$ $\left[\frac{kJ}{K \cdot mol}\right]$	$\tau_{max}[s]$
DMPC	296.81 ± 0.05	220 ± 11	23.5 ± 1
DMPC with 0,5mol-% gramicidin A	296.80 ± 0.05	230 ± 12	21.3 ± 1
DMPC with 1mol-% gramicidin A	296.80 ± 0.05	250 ± 13	22.1 ± 1
DMPC with 1,5mol-% gramicidin A	296.76 ± 0.05	122 ± 6	13.6 ± 1

Table 4.1: Experimental values of c_p and τ at T_m.

Sample	L $\left[10^8 \frac{J \cdot K}{s \cdot mol}\right]$	$\alpha \left[10^{-4} \frac{s \cdot mol \cdot K}{J}\right]$
DMPC	8.25 ± 0.38	1.07 ± 0.05
DMPC with 0,5mol-% gramicidin A	9.51 ± 0.41	0.93 ± 0.04
DMPC with 1mol-% gramicidin A	11.83 ± 0.64	0.74 ± 0.04
DMPC with 1,5mol-% gramicidin A	7.90 ± 0.57	1.11 ± 0.08

Table 4.2: Calculated values of the phenomenological coefficients L and α.

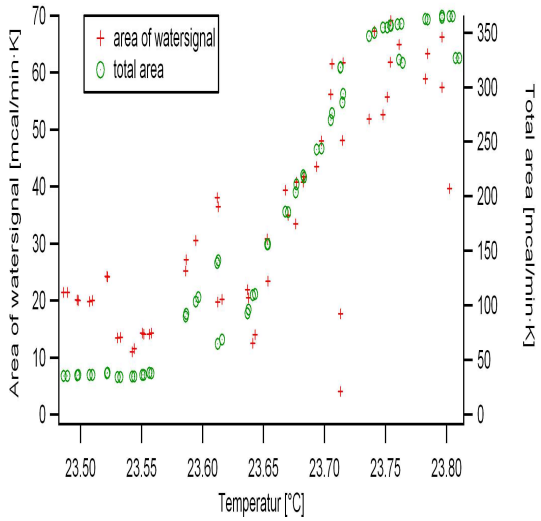

Figure 4.13: Water and total contribution. Areas calculated from negative pressure jumps on a DMPC sample.

Water contribution

Another aspect worth considering is the dependence of the areas of the lipid and water contributions on the temperature. When considering the theory, one would axpect the area of the lipid contribution to increase when going through the phase transition, whereas the contribution from the water fit should stay constant. This is, however, not the case.

In figure 4.13 the areas of the total signal and of the water contribution are plotted as functiontions of the temperature. Only negative pressurejumps are considered. One sees that the area of the water contribution increases with increasing temperature. The same tendency was exhibited by the other samples.

The area of the water response are almost 20% of the total contribution through the whole transition.

The most likely explanation of this is that the assumption of a single relaxation process is incorrect, that means that the eq. 4.5 is not the only equation describing the relaxation of the system, as mentioned in sec. 4.1.3. Thus, the increase of the contribution from the water signal might be an indication ofmore than a single relaxation in the process.

Yet, if one fills both cells of the pressure cell with distilled water and conducts pressure jumps at different temperatures, and fits the calorimeter response as done for the lipid containing samples, one also gets an increase of the water contribution with increasing temperature.

However, I do not have enough data on this to determine whether the increase in the water contribution is due to relaxation processes not encountered for in the fitting procedure, or it is a consequense of the dependence of the heat capacity of water on the temperature.

4.4 Error Sources

The preparation of the samples yields uncertainties in the concentration of the samples. This is probably the reason why we encountered lower transition enthalpies than expected, as mentioned in section 4.2.1. The difficult filling of the pressure cell is also an error source.

There were thermocouples inserted into the pressurecell at different times. This may have let impurities into the sample, which may have an influence on the measurements.

The pure DMPC samples and the samples with added gramicidin A were not prepared in the same way, as the samples containing gramicidin A was prepared using an organic solvent. This may have an influence on the measurements.

The fitting procedure also yields error sources. When fitting the measured responses to the eq. 4.4, there are often a scattering in the values obtained for almost similar start and end points of the fit interval. This is especially the case in the limits of the phase transition. This is taken in to account in the fitting of each pressure jump.

5 Discussion

The primary aim of this project was to conduct pressure jump experiments on lipid-peptide systems, in order to study the relaxation kinetics.

This has been done on pure DMPC and DMPC-Gramicidin A systems.

It has been shown that the insertion of gramicidin A into the lipid membrane does not only have an influence on the heat capacity profile, but also on the relaxation behavour of the lipid membrane. In particular, it has been shown that the lowering of the heat capacity profile is accompanied by a lowering of the relaxation time. That is, the statement of proportionality between c_p and τ is valid not only for a lipid membrane, but also for a lipid membrane with a transmembrane peptide inserted.

Thus, the experiments of this thesis shows that the theory presented in the paper by Grabitz et al.[1], is valid also for a DMPC-Gramicidin A system.

This raises the question whether this is in general true for lipid systems and peptides. It could be interesting to do the same experiments with a peripheral peptide, in order to see if such a peptide would cause the same influence on the heat capacity and the relaxation behaviour.

Also it could be interesting to improve the techniques in order to detect different relaxations. We have in the fitting procedure assumed a single relaxation process. But it is very likely that there are more than one relaxation process occuring during the phase transition. The formation of domains, as described with Monte-Carlo simulation could be one relaxation, whereas for instance the relaxation of the fatty acid chains could yield another relaxation time.

Outlook

Upon the finding that the presense of a transmembrane peptide can change both the relaxation time and the heat capacity profile of the lipid membrane, the question arises whether this is a phenomenon of relevance in biology.

The experiments in this thesis are performed on a simplified system which shows pronounced melting peaks, as this is necessary in order to resolve the relaxation time with the experimental equipment used.

The relaxation time of E. Coli has been approximated to be in the 10ms-100ms regime [1]. Many biological processes are assumed to take place in the same time regime. This leads to the thought that the relaxation time of the membrane could have a relation to the rate with wich biological processes related to the membrane are processed.

Many of the organelles in the biological cell are defined by lipid membranes. If it shows that there is a proportionality between the heatcapacity and the relaxation time also for biological membranes, this could be of significant importance for the understanding of biological systems. If the time rates of the processes are linked with the relaxation time of the lipid membrane, this would mean that one has to seek a thorough understanding of the lipid membrane in order to understand the processes in the cell.

Further, the connection between the relaxation and the formation of domains as simulated in the Monte-Carlo simulation could be interesting to investigate further, as the membrane shows different properties in the different states.

6 Acknowledgements

I would like to thank the members of the Membrane Biophysics and Thermodynamics Group at the Niels Bohr Institute for their help and good diskussions. Especially, I would like to thank Heiko Seeger for his invaluable help and guidance through the whole process.

References

[1] P. Grabitz, V.P. Ivanova, and T. Heimburg .(2002). Relaxation Kinetics of Lipid Membranes and its Relation to the Heat Capacity. Biophysical Journal. 82: 299-309.

[2] S.J. Singer and G. L. Nicolson. (1972). The fluid Mosaic Model of the Structure of Cell Membranes. Science. Vol. 175, 720-731

[3] J. Lee and J. M. Kosterlitz. (1991). Finite-size scaling and Monte Carlo simulations of first-order phase transitions. Phys. Rev. B. 43, 3265-3277

[4] H. Ebel, P. Grabitz and T. Heimburg. (2001). Enthalpy and volume changes in lipid membranes. I. the proportionality of heat and volume changes in the lipid melting transition and its implication for the elastic constants. J. Phys. Chem. B. 105, 7353-7360

[5] V.P. Ivanova, I.M. Makarow, T.E. Schäffer and T. Heimburg. (2003). Analyzing Heat Capacity Profiles of Peptide-Containing Membranes: Cluster Formation of Gramicidin A. Biophysical Journal. 84:2427-2439.

[6] T. Heimburg. (1998). Mechanical aspects of membrane thermodynamics. Estimation of mechanical properties of lipid membranes close to the chain melting transition form calorimetry. Biochim. Biophys. Acta. 1415: 147-162.

[7] V.P. Ivanova. (2000). Theoretical and experimental study of protein-lipid interactions. Phd. Thesis. Georg-August-Universität zu Göttingen.

[8] S. Doniac. (1973). Thermodynamic fluctuations in phopholipid bilayers. J. Chem. Phys. 68 : 4912-1916

[9] D. Pink, T. Green and D. Chapman. (1980).Raman Scattering in Bilayers of Saturated Phosphatidylcholines. Experiment and Theory.19:349-356

[10] T. Schlötzer. (2002). Masters Thesis. University of Göttingen.

[11] T. L. Hill. (1962). Introduction to Statistical Thermodynamics. 2nd printing. Addison-Wesley.

[12] I. Prigogine. (1998). Modern Thermodynamics: From Heat Engines to Dissipative Structures. John Wiley & Sons.

[13] T. Heimburg. (2004). Lecture Notes for the course "Biophysics of Membranes", University of Copenhagen.

[14] O.G. Mouriten et al.. (1983). Computer simulation og the main gel-fluid phase transition of lipid bilayers. J. Chem. Phys. 79: 2027-2041.